Physics Letters A 379 (2015) 2681–2684

Contents lists available at ScienceDirect

Physics Letters A

www.elsevier.com/locate/pla

Bounds on higher-order Lorentz-violating photon sector coefficients from an asymmetric optical ring resonator experiment

Stephen R. Parker [a,*], Matthew Mewes [b], Fred N. Baynes [a], Michael E. Tobar [a]

[a] School of Physics, The University of Western Australia, Crawley 6009, Australia
[b] California Polytechnic State University, San Luis Obispo, CA 93407, USA

ARTICLE INFO

Article history:
Received 10 July 2015
Received in revised form 3 August 2015
Accepted 4 August 2015
Available online 7 August 2015
Communicated by P.R. Holland

Keywords:
Lorentz invariance
Standard Model Extension
Optics
Resonators
Nonrenormalizable operators

ABSTRACT

Optical resonators provide a powerful tool for testing aspects of Lorentz invariance. Here, we present a reanalysis of an experiment where a path asymmetry was created in an optical ring resonator by introducing a dielectric prism in one arm. The frequency difference of the two fundamental counter-propagating modes was then recorded as the apparatus was orientation-modulated in the laboratory. By assuming that the minimal Standard-Model Extension coefficients vanish we are able to place bounds on higher-order parity-odd Lorentz-violating coefficients of the Standard-Model Extension. The results presented in this work set the first constraints on two previously unbounded linear combinations of $d = 8$ parity-odd nonbirefringent nondispersive coefficients of the photon sector.

1. Introduction

Lorentz invariance is a fundamental component of the Standard Model and General Relativity. Despite the successes of both theories they remain incompatible; it is generally assumed they are both low-energy approximations of a single theory that is consistent at the Planck scale [1]. Various efforts towards identifying a unified theory can allow or require Lorentz invariance to be broken [1,2]. Testing Lorentz invariance thus provides one of the few experimental portals for assessing and guiding theories of quantum gravity and other unification propositions. Precision laboratory measurements of Planck-scale suppressed effects offer excellent prospects in the search for Lorentz-Invariance Violations (LIV) [1].

The Standard-Model Extension (SME) provides a comprehensive framework for analyzing, quantifying and comparing different experimental tests of LIV [3–6]. The SME describes all possible Lorentz and *CPT* violations associated with known particles and fields. Efforts have usually focused on the minimal SME sectors, which only contain energy-independent operators of renormalizable dimension in flat spacetime. In recent years the SME has been expanded to include higher-order nonrenormalizable operators, which presents new opportunities for experimentation and analysis [7,8]. Bounds have previously been placed in the photon sector [9,10], with results in other sectors now starting to emerge [11,12]. Practically there are situations where one might expect LIV to manifest at higher-order, e.g. in some theories with noncommutative spacetime coordinates LIV only occurs for non-renormalizable operators [13,14].

In the photon sector of the SME operators can be classified into different groups that describe their effects on standard electrodynamics. Astrophysical observations have tightly constrained birefringent and vacuum dispersive effects with sensitivities far beyond the reach of terrestrial tests. This provides physical motivation to the study of the camouflage coefficients, which to leading order are nonbirefringent and nondispersive. The camouflage coefficients are *CPT* invariant, have even dimension $d \geq 4$, and are best constrained via precision electromagnetic resonant-cavity tests, such as the modern descendants of the Michelson–Morley experiment.

Constraints have previously been set on combinations of $d = 6$ and $d = 8$ camouflage coefficients using data from a parity-even microwave cavity experiment [9] and a parity-odd optical cavity experiment [10]. As the sensitivity to the camouflage coefficients scales with the frequency of the photon (roughly as ν^{d-4}), optical cavities are very well suited for testing these effects [8]. For the parity-odd camouflage coefficients there are three $d = 6$ coefficients and 13 $d = 8$ coefficients, with three linear combinations currently unbounded. Here we analyze an orientation modulated parity-odd asymmetric optical ring resonator experiment to set bounds on higher-order parity-odd camouflage coefficients, including the first constraints on two of the three remaining unbounded $d = 8$ combinations.

* Corresponding author.
E-mail address: stephen.parker@uwa.edu.au (S.R. Parker).

http://dx.doi.org/10.1016/j.physleta.2015.08.006
0375-9601/

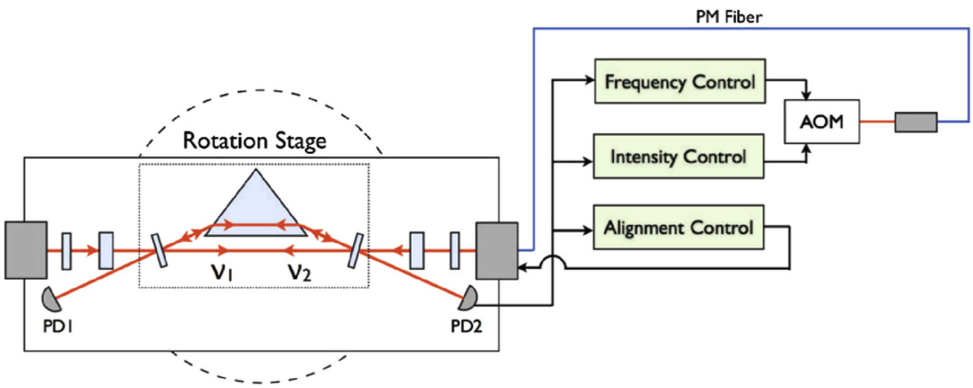

Fig. 1. Schematic of the parity-odd asymmetric optical ring resonator experiment, reproduced from [15]. This only shows the control systems and setup for one of the counter-propagating modes, there is a nominally identical setup for the second mode.

2. Experimental setup

A detailed overview of the experiment is provided in [16] and [15]. As seen in Fig. 1 a dielectric prism with index of refraction $n = 1.44$ is placed in one arm of an optical ring resonator to create a path asymmetry. A 1064 nm laser is split and each path is independently locked to a fundamental counter-propagating mode. The first laser path is frequency shifted by an Acousto-Optic Modulator (AOM), introducing a 160 MHz offset, and then mode-locked by applying correction signals to the laser. The second path is locked to the counter-propagating mode via an AOM; the correction signal contains the frequency difference (typically ∼100 Hz) of the two modes imprinted on the 160 MHz offset. This was recorded directly with a frequency counter.

The apparatus sits upon a rotation platform. The beat frequency was recorded for 10 minutes in a stationary position, then the experiment was rotated by +180° and the beat frequency recorded for 10 minutes while stationary. The experiment was then rotated back by −180° to the initial position and the cycle repeated. The result of this is that the final dataset is in essence stationary, but with leading-order noise processes shifted to a different frequency. Previously, measurements were made for 50 days and used to place bounds in the minimal SME [15]. We use the same dataset for the following analysis, but assume that the minimal SME terms vanish.

3. Experimental sensitivity to higher-order camouflage coefficients

A complete derivation of the camouflage coefficients is provided in [7]. In short, the coefficients associated with *CPT*-even differential operators from the arbitrary Lorentz and *CPT* violating Lagrange density for photon propagation are decomposed via spin-weighted spherical harmonics. This then allows for groups of coefficients associated with different physical properties to be collected together. The coefficients from operators with no leading-order birefringence are denoted $(c_F^{(d)})^{(0E)}_{njm}$, where d is the mass dimension, 0 is the spin weight, $E = (-1)^j$ is the parity, n is the wavelength dependence, j is the total angular momentum and m is the z-component of angular momentum. The camouflage coefficients are then the subset of $(c_F^{(d)})^{(0E)}_{njm}$ coefficients that are not associated with leading-order vacuum dispersion,

$$(c_F^{(d)})^{(0E)}_{njm} = (\bar{c}_F^{(d)})^{(0E)}_{njm} - (\bar{c}_F^{(d)})^{(0E)}_{(n-2)jm}.$$

Here, we restrict our attention to $d = 6, 8$, with $0 \le n \le (d-4)$, $j = n, n-2, \ldots \ge 0$ and $|m| \le j$. For coefficients with $m \ne 0$ there are real and imaginary components.

The measured fractional beat frequency between the two counter-propagating modes of Fig. 1 is

$$\frac{\nu_{\text{beat}}}{\nu} = \sum_{mm'} A_{mm'} e^{im\phi + im'\omega_\oplus T_\oplus}, \tag{1}$$

where ϕ is the angle between the laboratory-frame x axis and geographical south, $\omega_\oplus$ is the Earth's sidereal rotation rate and $T_\oplus$ is the sidereal time since the last alignment of the experiment with the Sun-Centered Celestial Equatorial Frame (SCCEF), the conventional choice of reference frame for analysis of such experiments within the SME [5]. The $A_{mm'}$ factors contain linear combinations of Lorentz-violating coefficients that a given experiment is sensitive to. They satisfy the relationship $A^*_{mm'} = A_{(-m)(-m')}$ and can be calculated from

$$A_{mm'} = \sum_{dnj} \Delta M^{(d)lab}_{njm} d^{(j)}_{mm'}(-\chi)(\bar{c}_F^{(d)})_{njm'}. \tag{2}$$

Here $\Delta M^{(d)lab}_{njm}$ is an experiment-dependent constant that considers the difference between the two counter-propagating modes of Fig. 1, $d^{(j)}_{mm'}$ are the little Wigner matrices and χ is the co-latitude of the experiment. A detailed guide describing these factors and how to calculate them is provided in Section IV of [8].

As is standard for the analysis of turntable experiments [9,17] we can model the data as

$$\frac{\nu_{\text{beat}}}{\nu} = \sum_{m\ge 0} C_m \cos(m\phi) + S_m \sin(m\phi), \tag{3}$$

$$C_m = \sum_{m'\ge 0} C^C_{mm'} \cos\left(m'\omega_\oplus T_\oplus\right) + C^S_{mm'} \sin\left(m'\omega_\oplus T_\oplus\right), \tag{4}$$

$$S_m = \sum_{m'\ge 0} S^C_{mm'} \cos\left(m'\omega_\oplus T_\oplus\right) + S^S_{mm'} \sin\left(m'\omega_\oplus T_\oplus\right), \tag{5}$$

with the cosine and sine amplitudes of Eqs. (4) and (5) given by

$$C^C_{mm'} = 2\eta_m\eta_{m'} \operatorname{Re}(A_{mm'} + A_{m(-m')}),$$
$$C^S_{mm'} = -2\eta_m \operatorname{Im}(A_{mm'} - A_{m(-m')}),$$
$$S^C_{mm'} = -2\eta_{m'} \operatorname{Im}(A_{mm'} + A_{m(-m')}), \tag{6}$$
$$S^S_{mm'} = -2 \operatorname{Re}(A_{mm'} - A_{m(-m')}), \tag{7}$$

with $\eta_0 = 1/2$ and $\eta_m = 1$ for all other values. Despite the experiment being mounted on a turntable the dataset is effectively stationary with the experiment x-axis permanently aligned parallel to East–West, thereby setting $\phi = \pi/2$. This sets the cosine component of Eq. (3) to zero, so experimental access to Lorentz violating